Inorg. Chem. **2007**, *46*, 11145–11155

Rates of Proton Transfer to Fe–S-Based Clusters: Comparison of Clusters Containing $\{MFe(\mu_2\text{-}S)_2\}^{n+}$ and $\{MFe_3(\mu_3\text{-}S)_4\}^{n+}$ (M = Fe, Mo, or W) Cores

Katie Bates, Brendan Garrett, and Richard A. Henderson*

Chemistry, School of Natural Sciences, University of Newcastle, Newcastle upon Tyne, NE1 7RU, United Kingdom

Received August 3, 2007

The rates of proton transfer from $[pyrH]^+$ (pyr = pyrrolidine) to the binuclear complexes $[Fe_2S_2Cl_4]^{2-}$ and $[S_2MS_2FeCl_2]^{2-}$ (M = Mo or W) are reported. The reactions were studied using stopped-flow spectrophotometry, and the rate constants for proton transfer were determined from analysis of the kinetics of the substitution reactions of these clusters with the nucleophiles Br^- or PhS^- in the presence of $[pyrH]^+$. In general, Br^- is a poor nucleophile for these clusters, and proton transfer occurs before Br^- binds, allowing direct measure of the rate of proton transfer from $[pyrH]^+$ to the cluster. In contrast, PhS^- is a better nucleophile, and a pathway in which PhS^- binds preferentially to the cluster prior to proton transfer from $[pyrH]^+$ usually operates. For the reaction of $[Fe_2S_2Cl_4]^{2-}$ with PhS^- in the presence of $[pyrH]^+$ both pathways are observed. Comparison of the results presented in this paper with analogous studies reported earlier on cuboidal Fe–S-based clusters allows discussion of the factors which affect the rates of proton transfer in synthetic clusters including the nuclearity of the cluster core, the metal composition, and the nature of the terminal ligands. The possible relevance of these findings to the protonation sites of natural Fe–S-based clusters, including FeMo-cofactor from nitrogenase, are presented.

Introduction

Proton transfer is a reaction ubiquitous in chemistry and biology, and understanding the factors controlling the rates of these reactions is fundamental to a wide range of complex processes.[1] Often proton-transfer reactions comprise part of a multistep process (e.g., in the reactions of enzymes), and in these cases understanding the protonation step has to rely on established chemical precedent from studies on simpler synthetic analogues of the active site.

Fe−S-based clusters constitute the active site in a wide range of proteins.[2] The composition and structures of the clusters are varied and reflect the role of the protein: from electron-transfer agents to the active site in enzymes such as aconitase, hydrogenases, nitrogenases, carbon monoxide dehydrogenase, and sulfite reductase. In some proteins containing Fe−S-based clusters, protonation of the cluster is implicated in its reaction and theoretical studies have been used to investigate the mechanism and probe where protons bind to the cluster.[3] Our kinetic studies on synthetic Fe−S-based clusters complement these theoretical studies on the protonation of natural Fe−S-based clusters, and we will compare the experimental and theoretical findings later in this paper.

In a series of studies we developed kinetic methods for measuring the proton affinities[4] and (more recently) rates of proton transfer of synthetic Fe−S-based clusters.[5] Early studies focused on measuring the proton affinities of the

(1) See articles in *Recent Advances in Hydride Chemistry*; Peruzzini, M., Poli, R., Eds.; Elsevier: Amsterdam, 2001; notably Chapters 2 and 16.

(2) Lee, S. C.; Holm, R. H. *Chem. Rev.* **2005**, *104*, 135 and references therein.

(3) (a) Dance, I. *Aust. J. Chem*. **1994**, *47*, 979. (b) Dance, I. *Chem. Commun*. **1997**, 165. (c) Dance, I. *Chem. Commun*. **1998**, 523. (d) Lovell, T.; Li, J.; Liu, T.; Case, D. A.; Noodleman, L. *J. Am. Chem. Soc*. **2001**, *123*, 12392. (e) Lovell, T.; Li, J.; Case, D. A.; Noodleman, L. *J. Am. Chem. Soc*. **2002**, *124*, 4546. (f) Lovell, T.; Torres, R. A.; Hau, W. G.; Liu, T.; Case, D. A.; Noodleman, L. J. *J. Biol. Inorg. Chem.* **2002**, *7*, 735. (g) Durrant, M. C. *Biochemistry* **2002**, *41*, 13934. (h) Durrant, M. C. *Biochemistry* **2002**, *41*, 13946. (i) Hunter, U.; Ahlrichs, R.; Coucouvanis, D. *J. Am. Chem. Soc*. **2004**, *126*, 2588.

(4) (a) Henderson, R. A. *Chem. Rev.* **2005**, *105*, 2365 and references therein. (b) Henderson, R. A. *Coord. Chem. Rev.* **2005**, *249*, 1841 and references therein.

(5) (a) Henderson, R. A.; Oglieve, K. E. *J. Chem. Soc., Dalton Trans.* **1999**, 3927. (b) Bell, J.; Dunford, A. J.; Hollis, E.; Henderson, R. A. *Angew. Chem., Int. Ed*. **2003**, *42*, 1149. (c) Dunford, A. J.; Henderson, R. A. *J. Chem. Soc., Dalton Trans*. **2002**, 2837.

10.1021/ic7015484 CCC: $37.00
Published on Web 11/29/2007

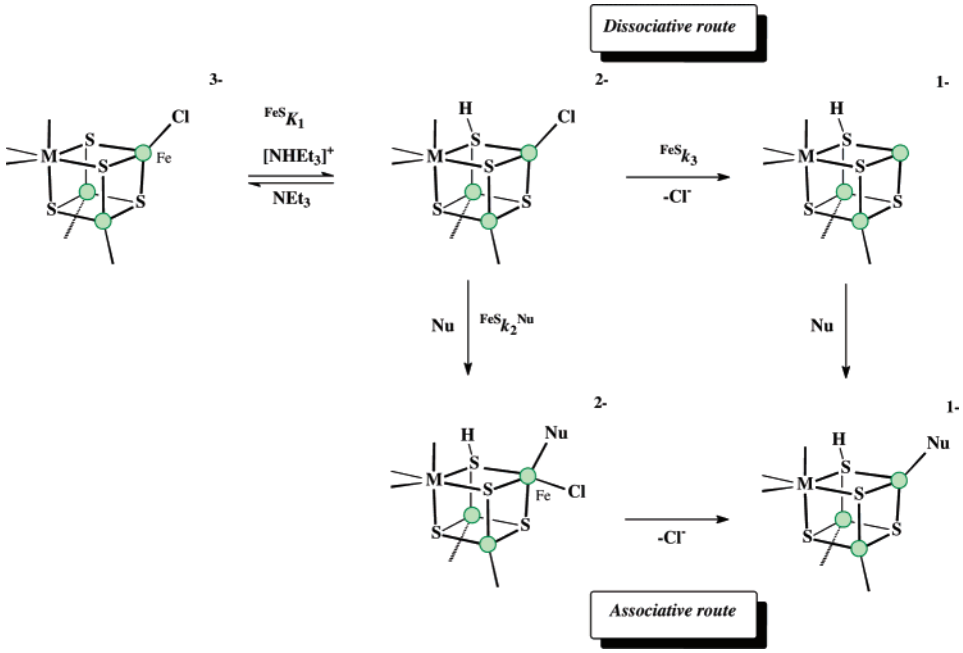

Figure 1. Acid-catalyzed substitution pathways for the reaction of synthetic Fe−S-based clusters.

clusters by measuring the effect that acid has on the rates of substitution in MeCN. These studies employed acids such as $[NHEt_3]^+$ (pK_a = 18.46 in MeCN)[6] which protonate the clusters rapidly prior to the act of rate-limiting substitution. Consequently, these reactions are best classified as acid-catalyzed substitution reactions and operate by the pathways summarized in Figure 1. Analysis of the kinetic data from such reactions show the following characteristics. (i) Protonation affects the rate of substitution. (ii) Single protonation occurs on the cluster. (iii) The pK_a of essentially all synthetic Fe−S-based clusters fall in the narrow range 17.9−18.9 in MeCN irrespective of the metal composition, terminal ligands, or charge on the cluster.

In these acid-catalyzed substitution reactions using $[NHEt_3]^+$ the rates of protonation of the clusters are fast and the act of substitution is invariably rate limiting. By using the much weaker acid $[pyrH]^+$ (pyr = pyrrolidine; pK_a = 21.5 in MeCN)[6] proton transfer to the clusters becomes thermodynamically unfavorable and hence sufficiently slow to allow us to investigate how the rates of proton transfer are affected by the composition of the cluster.

Although there have been only a few measurements of the rates of proton transfer to synthetic Fe−S-based clusters, some characteristics are already clear. First, protonation of synthetic Fe−S-based clusters is significantly slower than the diffusion-controlled limit, even for thermodynamically favorable reactions. Furthermore, in contrast to the pK_a's of the clusters the rates of proton transfer are sensitive to the metal composition and ligation of the cluster. Our ultimate aim is to delineate the factors that control the rates of proton transfer to synthetic Fe−S-based clusters. To this end, we present herein kinetic studies on the proton transfer to synthetic Fe−S-based clusters with a binuclear core composition $\{MFeS_2\}^{n+}$ (M = Fe, Mo, or W) containing μ_2-S. Comparison of the results presented herein with those for cuboidal clusters with core composition $\{MFe_3S_4\}^{3+}$ (M = Fe, Mo),[5] containing μ_3-S, allows us to investigate how changing the metal composition, terminal ligands, and nuclearity of the cluster affect the rates of proton transfer.

(6) Izutsu, K. *Acid-Base Dissociation Constants in Dipolar Aprotic Solvents*; Blackwells Scientific: Oxford, 1990.

Results and Discussion

Although protonation is a reaction common to essentially all synthetic Fe−S-based clusters, direct detection of protons bound to Fe−S-based clusters has, so far, not proved possible. However, it is evident that these clusters protonate from the way in which acids affect the rates of reactions involving replacement of terminal ligands. It seems most likely that the protonation is at a μ-S site although, at the moment, there is no unambiguous proof of this proposal.

The protonation reactions of synthetic Fe−S-based clusters are sufficiently fast to require use of stopped-flow spectrophotometry. However, these reactions are invariably associated with negligible changes in the UV−visible spectrum, and the reasons for this have been discussed before.[4,5] This means that we cannot study protonation reactions directly. In contrast, substitution of the terminal ligands of Fe−S-based clusters are usually associated with significant changes in the electronic spectrum. Consequently, it has been necessary to investigate the protonation of Fe−S-based clusters indirectly by analyzing the effect that acid has on the rate of substitution of terminal ligands. Effectively, the rates of the substitution reactions act as a "reporter" on the protonation state of the cluster.

In the presentation of our results on the reactions of $[Fe_2S_2Cl_4]^{2-}$ and $[S_2MS_2FeCl_2]^{2-}$ (M = Mo or W) with $[pyrH]^+$ which follows we will first present the kinetic studies on the binuclear complexes and then discuss the general features which have emerged from these studies.

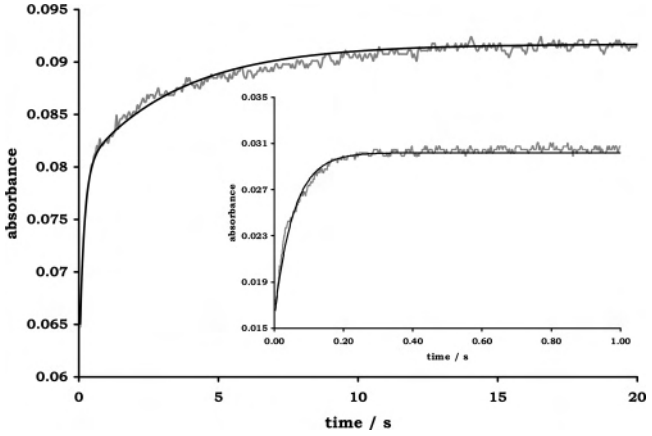

Figure 2. Typical stopped-flow absorbance−time traces (grey lines) and fits (black lines) for the reactions of $[Fe_2S_2Cl_4]^{2-}$ with $[pyrH]^+$ in the presence of (main) PhS^- ($[pyrH^+] = 0.5$ mmol dm^{-3}, $[PhS^-] = 10$ mmol dm^{-3}; measured at $\lambda = 550$ nm; curve fit $A_t = 0.0918 - 0.018e^{-6.1t} - 0.012e^{-0.29t}$), and (insert) Br^- ($[pyrH^+] = 10$ mmol dm^{-3}, $[Br^-] = 10$ mmol dm^{-3}; measured at $\lambda = 400$ nm; curve fit $A_t = 0.0302 - 0.0143e^{-18.1t}$).

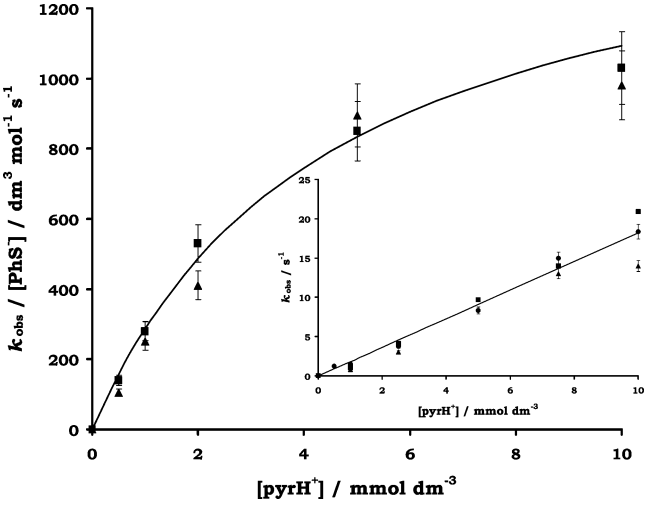

Figure 3. Kinetics of the reaction between $[Fe_2S_2Cl_4]^{2-}$ (0.1 mmol dm^{-3}) and PhS^- in the presence of $[pyrH]^+$ in MeCN at 25.0 °C. Data show the dependence of $k_{obs}/[PhS^-]$ on the concentration of $[pyrH]^+$. The data points correspond to $[PhS^-] = 20$ (▲) and 10 mmol dm^{-3} (■). Error bars indicate ±10% reproducibility. (Insert) Kinetics of the reaction between $[Fe_2S_2Cl_4]^{2-}$ and Br^- in the presence of $[pyrH]^+$ in MeCN at 25.0 °C. Data show the dependence of k_{obs} on the concentration of $[pyrH]^+$. The data points correspond to $[Br^-] = 20$ (▲), 10 (●), and 5 mmol dm^{-3} (■). Error bars indicate ±5% reproducibility. Line drawn is that defined by eq 2.

Basicity of Binuclear Clusters. The proton affinities of $[Fe_2S_2Cl_4]^{2-}$ (p$K_a = 18.1$),[7] $[S_2MoS_2FeCl_2]^{2-}$ (p$K_a = 17.9$), and $[S_2WS_2FeCl_2]^{2-}$ (p$K_a = 18.1$)[8] in MeCN have been reported earlier. Interestingly, the pK_a of $[Fe_2S_2Cl_4]^{2-}$ is similar to, but slightly less than, that of $[Fe_4S_4Cl_4]^{2-}$ (18.8).[8] Intuitively, it might be anticipated that μ_2-S (bound to two Fe^{3+} atoms) would be more basic than μ_3-S (bound to three $Fe^{2.5+}$ atoms). That the two types of sulfur in these clusters have such similar basicities is perhaps indicative that the bonding between Fe and S involves both S-to-Fe σ-donation and Fe-to-S π-backbonding.[9] The overall effect is that a μ_2-S ligated by two $FeCl_2$ residues has a similar basicity to a μ_3-S ligated by three FeCl residues.

While the basicity of the core sulfurs in synthetic Fe−S-based clusters is remarkably insensitive to the cluster nuclearity, metal composition, terminal ligands, and overall charge, earlier studies indicate that for cuboidal clusters the rates of proton transfer are markedly dependent on all these factors.[4,5] This observation is further substantiated in the results of the kinetic studies on the reactions of $[pyrH]^+$ with $[Fe_2S_2Cl_4]^{2-}$ or $[S_2MS_2FeCl_2]^{2-}$ described below.

Before presenting and discussing the kinetic data it is important to stress that, in line with earlier studies on Fe−S-based clusters, we will only consider the first acts of substitution. Clearly in $[Fe_2S_2Cl_4]^{2-}$ there are four chloro groups to be substituted, while in $[S_2MS_2FeCl_2]^{2-}$ there are two chloro groups to be substituted. For both types of clusters, in the reactions involving Br^- as nucleophile, the stopped-flow absorbance−time traces can be fitted to single-exponential curves as shown in Figure 2, presumably because the first act of substitution is the slowest. However, substitution reactions of these same clusters involving PhS^- as nucleophile are associated with biphasic absorbance−time curves (Figure 2) with both phases showing analogous dependences on concentrations of acid and thiolate. The whole trace corresponds to substitution of all Fe−Cl groups in the cluster. This biphasic behavior could be attributable to statistical kinetics. However, an alternative[4] explanation is that the first phase corresponds to the first act of substitution, the second phase to the second act of substitution, and subsequent substitution steps are either fast or the absorbance changes associated with the later substitution steps are too small to be detectable. In order to compare the results from the studies with the two nucleophiles we only consider the kinetics of the first phase for the studies with PhS^- in the discussion presented below. However, in the Supporting Information the observed rate constants for both phases (k_{obs1} and k_{obs2}) of the reactions of $[Fe_2S_2Cl_4]^{2-}$ and $[S_2MS_2FeCl_2]^{2-}$ (M = Mo or W) with $[pyrH]^+$ in the presence of PhS^- are presented.

Rates of Proton Transfer to $[Fe_2S_2Cl_4]^{2-}$. The kinetics of the reaction between $[Fe_2S_2Cl_4]^{2-}$ and Br^- in the presence of $[pyrH]^+$ is shown in Figure 3 (insert). The kinetics exhibit a first-order dependence on the concentration of $[pyrH]^+$ but are independent of the concentration of Br^-. The experimental rate law is shown in eq 1. These kinetics are consistent with the mechanism shown in the bottom line of Figure 4 ($Nu^- = Br^-$), where protonation of the cluster occurs before Br^- can bind. The studies with Br^- gives the rate constant for protonation of $[Fe_2S_2Cl_4]^{2-}$ by $[pyrH]^+$ ($^{Fe2}k_1 = (1.8 \pm 0.2) \times 10^3$ dm^3 mol^{-1} s^{-1}). The independence of the reaction rate on the concentration of Br^- indicates that in the substitution step Br^- binds to the cluster after protonation

$$\frac{-d[Fe_2S_2Cl_4^{2-}]}{dt} = (1.8 \pm 0.2) \times 10^3[pyrH^+][Fe_2S_2Cl_4^{2}] \quad (1)$$

The bottom pathway in Figure 4 shows the mechanism for the reaction between $[Fe_2S_2Cl_4]^{2-}$ and $[pyrH]^+$ in the

(7) Henderson, R. A.; Oglieve, K. E. *Chem. Commun.* **1994**, 1961.
(8) Almeida, V. R.; Gormal, C. A.; Gronberg, K. L. C.; Henderson, R. A.; Oglieve, K. E.; Smith, B. E. *Inorg. Chim. Acta* **1999**, *291*, 212.
(9) Sellmann, D.; Sutter, J. *Acc. Chem. Res.* **1997**, *30*, 460.

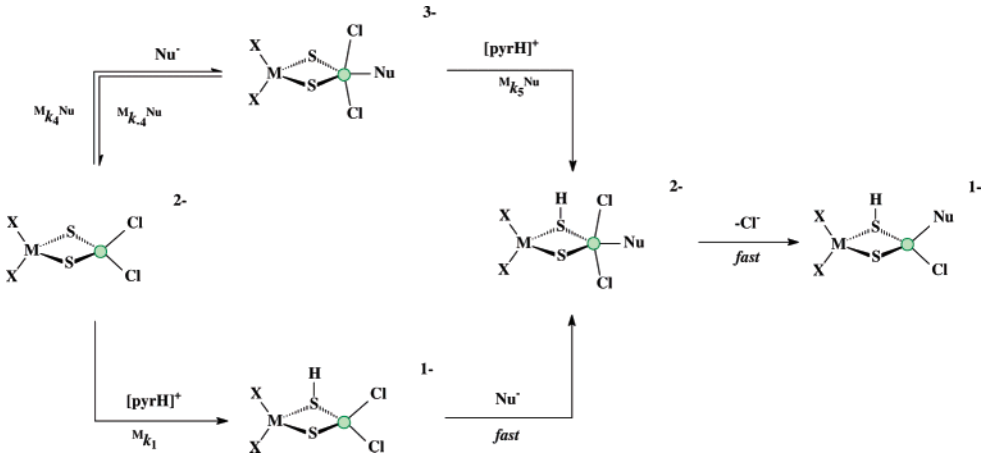

Figure 4. Mechanisms involving substitution and protonation steps for the reactions of $[Fe_2S_2Cl_4]^{2-}$ ($MX_2 = FeCl_2$) or $[S_2MS_2FeCl_2]^{2-}$ ($MX_2 = MoS_2$ or WS_2) with nucleophiles ($Nu^- = PhS^-$ or Br^-) in the presence of $[pyrH]^+$.

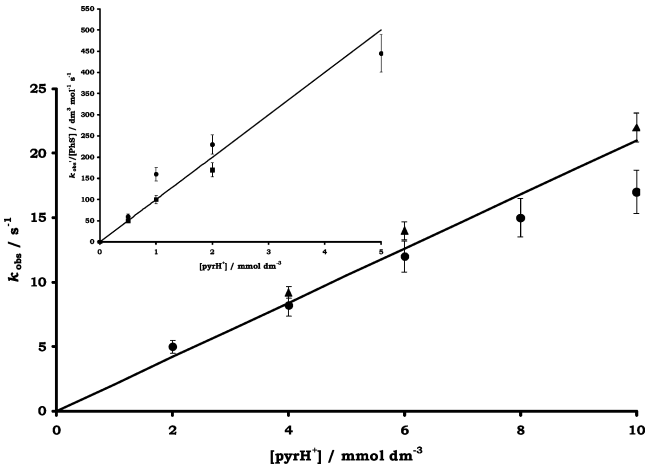

Figure 5. Kinetics of the reaction between $[Fe_2S_2Cl_4]^{2-}$ (0.1 mmol dm^{-3}) and PhS^- in the presence of $[pyrH]^+$ in MeCN at 25.0 °C. Data show the dependence of k_{obs} on the concentration of $[pyrH]^+$ when $[PhS^-] = 1$ mmol dm^{-3} (▲) and $[PhS^-] = 2$ mmol dm^{-3} (●). Error bars indicate ±10% reproducibility. Line drawn is that defined by eq 3. (Insert) Kinetics of the reaction between $[Fe_2S_2Cl_4]^{2-}$ (0.1 mmol dm^{-3}) and PhS^- in the presence of $[pyrH]^+$ in MeCN at 25.0 °C after correcting for the $^{Fe2}k_1$ pathway ($k_{obs'} = k_{obs} - {}^{Fe2}k_1[pyrH^+]$). Data presented correspond to $[PhS^-] = 20$ (▲) and 10 mmol dm^{-3} (■). Error bars indicate ±10% reproducibility. Line drawn is that defined by eq 4 and the parameters presented in the text.

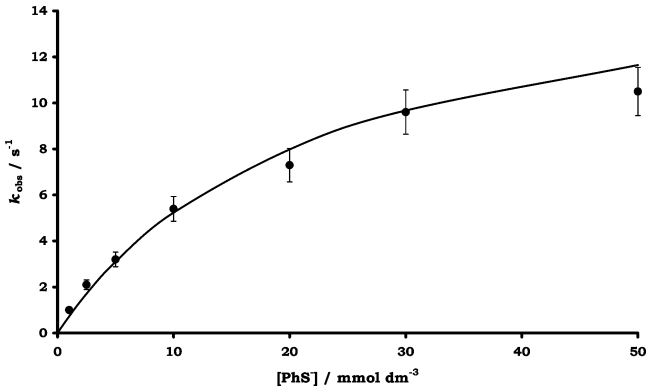

Figure 6. Kinetics of the reaction between $[Fe_2S_2Cl_4]^{2-}$ (0.1 mmol dm^{-3}) and PhS^- in MeCN at 25.0 °C. Error bars indicate ±10% reproducibility. Curve drawn is that defined by eq 5.

presence of a nucleophile which binds more slowly to the cluster than the rate of protonation of the cluster by $[pyrH]^+$. It seems likely that with other nucleophiles binding of the nucleophile could be faster than proton transfer. We will elaborate on this further in the context of the reaction with PhS^-.

The kinetics of the reaction between $[Fe_2S_2Cl_4]^{2-}$ and PhS^- in the presence of $[pyrH]^+$ in MeCN as solvent are shown in Figure 3 (main part). The values of k_{obs} presented in Figure 3 correspond to only the acid-dependent reaction. The experimentally observed rate constants (see Supporting Information) correspond to both the acid-dependent and the acid-independent rates (vide infra, see Figure 6). In order to produce the data presented in Figure 3 (main) the rate of the acid-independent pathway has been subtracted from the experimentally observed rate constant.

The acid-dependent reaction exhibits a first-order dependence on the concentration of PhS^- and an apparent complicated dependence on the concentration of $[pyrH]^+$. At low concentrations of $[pyrH]^+$ the rate exhibits a first-order dependence on the concentration of acid, but at high concentrations of $[pyrH]^+$ the rate is independent of the concentration of acid. It is important to note that in MeCN solutions the protolytic equilibrium shown in eq 2 between $[pyrH]^+$ ($pK_a = 21.5$ in MeCN)[6] and PhS^- ($pK_a \geq 19.3$ in MeCN)[5a] lies to the left-hand side ($K_0 < 6.3 \times 10^{-3}$). Earlier studies[5a] have shown that in such mixtures negligible amounts of PhSH are produced. Consequently, no correction to the concentrations of PhS^- or $[pyrH]^+$ has been applied.

$$PhS^- + [pyrH]^+ \overset{K_0}{\rightleftharpoons} PhSH + pyr \qquad (2)$$

The kinetics shown in Figure 3 (main) are similar to those observed in analogous studies on cuboidal Fe−S-based clusters,[5b] which were analyzed using a plot[10] of $[PhS^-]/k_{obs}$ vs $1/[pyrH^+]$ to give the experimental rate law consistent with the mechanism shown in the top line of Figure 4 ($Nu^- = PhS^-$). However, in the reaction of $[Fe_2S_2Cl_4]^{2-}$ with PhS^- in the presence of $[pyrH]^+$ the analysis is not so simple.

Consider *both* pathways shown in Figure 4. Which pathway the reaction employs depends on the relative rates of nucleophile binding ($^{Fe2}k_4^{PhS}[Nu]$) and protonation ($^{Fe2}k_1$-

(10) Wilkins, R. G. *Kinetics and Mechanisms of Reactions of Transition Metal Complexes*; VCH: Weinheim, Germany, 1991; p 23.

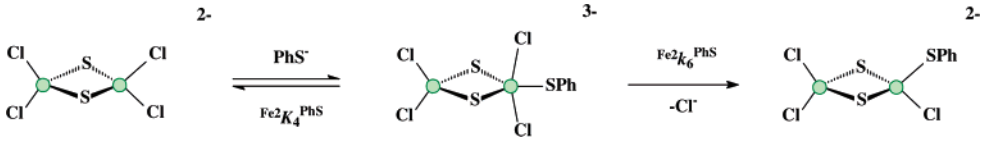

Figure 7. Mechanism for the substitution reaction between $[Fe_2S_2Cl_4]^{2-}$ and PhS^- in the absence of acids.

$[pyrH^+]$). If ${}^{Fe2}k_4{}^{PhS}$ and ${}^{Fe2}k_1$ are similar then which pathway operates will depend on the relative concentrations of PhS^- and $[pyrH]^+$. The kinetic data presented in Figure 3 (main) were collected (with the one exception when $[PhS^-] = [pyrH^+] = 10$ mmol dm^{-3}) under the condition $[PhS^-] > [pyrH^+]$. It would be anticipated that if ${}^{Fe2}k_4{}^{PhS}$ and ${}^{Fe2}k_1$ are similar and $[PhS^-] < [pyrH^+]$ then the rate of thiolate binding to $[Fe_2S_2Cl_4]^{2-}$ would be slower than the rate of proton transfer from $[pyrH]^+$ to $[Fe_2S_2Cl_4]^{2-}$, resulting in a change of the kinetics with the rate of proton transfer from $[pyrH]^+$ to $[Fe_2S_2Cl_4]^{2-}$ (${}^{Fe2}k_1$) becoming rate limiting. Figure 5 (main) shows the kinetics under such conditions. Only limited data is presented in Figure 5 because of the necessary experimental conditions that $[PhS^-] < [pyrH^+]$ and that the concentrations of both PhS^- and $[pyrH]^+$ must be in a large excess over the concentration of $[Fe_2S_2Cl_4]^{2-}$. Figure 5 (main) shows that when $[PhS^-] < [pyrH^+]$, the kinetics exhibit a linear dependence on $[pyrH^+]$ and are independent of the concentration of PhS^-. The straight line shown in Figure 5 is that defined by eq 3 with ${}^{Fe2}k_1 = (2.1 \pm 0.2) \times 10^3$ dm^3 mol^{-1} s^{-1}. The values of ${}^{Fe2}k_1$ established from the studies with Br^- and PhS^- are in excellent agreement.

$$\frac{-\mathrm{d}[Fe_2S_2Cl_4{}^{2-}]}{\mathrm{d}t} = {}^{Fe2}k_1\,[pyrH^+][Fe_2S_2Cl_4{}^{2-}] \qquad (3)$$

In earlier studies[5c] we showed that for both $[Fe_4S_4Cl_4]^{2-}$ and $[\{MoFe_3S_4Cl_3\}_2(\mu\text{-SR})_3]^{3-}$ the values of ${}^{FeS}k_4{}^{PhS}$ and ${}^{FeS}k_1$ are significantly different $({}^{FeS}k_4{}^{PhS})/({}^{FeS}k_1) = 6 - 1320$. However, the change in the kinetics for the reaction of $[Fe_2S_2Cl_4]^{2-}$ with PhS^- in the presence of $[pyrH]^+$ indicates that the values of ${}^{Fe2}k_4{}^{PhS}$ and ${}^{Fe2}k_1$ are sufficiently close that both the top and the bottom pathways of Figure 4 can operate concurrently.

We are now in a position to consider the data in Figure 3 (main) in more detail. It is clear that these data actually correspond to the sum of both the top and the bottom pathways in Figure 4. If we subtract the contribution of the ${}^{Fe2}k_1$ pathway from the data in Figure 3 (main) ($k_{obs'} = k_{obs} - {}^{Fe2}k_1[pyrH^+]$) then the residual rate corresponds to the contribution from the PhS^--dependent pathway (top pathway in Figure 4). It is important to stress that, in practice, this analysis is not simple. Even at high concentrations of PhS^-, the ${}^{Fe2}k_1$ pathway dominates at high concentrations of $[pyrH]^+$ and when $[pyrH^+] = 10$ mmol dm^{-3} the value of $k_{obs'} = k_{obs} - {}^{Fe2}k_1[pyrH^+]$ is small and very sensitive to the error in determining k_{obs}. The problems in this analysis are compounded further by the following: (i) k_{obs} has already been corrected for the PhS^--independent pathway (vide supra) and (ii) the values of k_{obs} for the reactions in the presence of PhS^- are determined from analysis of biphasic absorbance−time traces and are consequently associated with higher uncertainty than analysis of monophasic traces.

Because of all these problems we restricted our analysis to data collected at high concentrations of PhS^- ($[PhS^-] = 10$ or 20 mmol dm^{-3}) and $[pyrH^+] \le 5$ mmol dm^{-3}. The analysis is presented in Figure 5 (insert) and shows that after correcting for the ${}^{Fe2}k_1$ pathway the residual rate exhibits a first-order dependence on the concentrations of PhS^- and $[pyrH]^+$. The scatter in the data is because of the problems with the analysis outlined above, and the slight curvature at high concentrations of $[pyrH]^+$ in Figure 5 (insert) could be due to uncertainties in the analysis (even when $[pyrH^+] = 5$ mmol dm^{-3}), and hence, we are cautious of fitting the data to a curve.

The rate law for the top pathway in Figure 4 is presented in eq 4. The plot shown in Figure 5 (insert) is consistent with this rate law if ${}^{Fe2}k_{-4}{}^{PhS} > {}^{Fe2}k_5{}^{PhS}[pyrH^+]$. From the fit shown in Figure 5 (insert) we can calculate ${}^{Fe2}K_4{}^{PhS}({}^{Fe2}k_5{}^{PhS}) = 1 \times 10^5$ dm^6 mol^{-2} s^{-1} (where ${}^{Fe2}K_4{}^{PhS} = {}^{Fe2}k_4{}^{PhS}/{}^{Fe2}k_{-4}{}^{PhS}$).

$$\frac{-\mathrm{d}[Fe_2S_2Cl_4{}^{2-}]}{\mathrm{d}t} = \frac{{}^{Fe2}k_4{}^{PhS}({}^{Fe2}k_5{}^{PhS})[pyrH^+][PhS^-]}{{}^{Fe2}k_{-4}{}^{PhS} + {}^{Fe2}k_5{}^{PhS}[pyrH^+]}[Fe_2S_2Cl_4{}^{2-}] \qquad (4)$$

We also studied the kinetics of the reaction between $[Fe_2S_2Cl_4]^{2-}$ and PhS^- in the absence of acid to form $[Fe_2S_2(SPh)Cl_3]^{2-}$, and this together with the results presented above allow us to calculate the value of ${}^{Fe2}k_5{}^{PhS}$. The kinetics of the reaction between $[Fe_2S_2Cl_4]^{2-}$ and PhS^- exhibit a first-order dependence on the concentration of cluster and a nonlinear dependence on the concentration of PhS^- as shown in Figure 6. Analysis of the data yields the experimental rate law shown in eq 5. This rate law is consistent with the mechanism shown in Figure 7. The mechanism in Figure 7 is analogous to that described for substitution reactions of other Fe−S-based clusters and involves initial rapid binding of PhS^- to an Fe site followed by rate-limiting dissociation of an Fe−Cl bond. The mechanism in Figure 7 is associated with the rate law shown in eq 6. Comparison of eqs 5 and 6 yields ${}^{Fe2}K_4{}^{PhS} = 40.2 \pm 5$ dm^3 mol^{-1} and ${}^{Fe2}k_6{}^{PhS} = 18.0 \pm 3$ s^{-1}.

$$\frac{-\mathrm{d}[Fe_2S_2Cl_4{}^{2-}]}{\mathrm{d}t} = \frac{(7.24 \pm 0.3) \times 10^2[PhS^-]}{1 + (40.2 \pm 5)[PhS^-]}[Fe_2S_2Cl_4{}^{2-}] \qquad (5)$$

$$\frac{-\mathrm{d}[Fe_2S_2Cl_4{}^{2-}]}{\mathrm{d}t} = \frac{{}^{Fe2}K_4{}^{PhS}({}^{Fe2}k_6{}^{PhS})[PhS^-]}{1 + {}^{Fe2}K_4{}^{PhS}[PhS^-]}[Fe_2S_2Cl_4{}^{2-}] \qquad (6)$$

Since ${}^{Fe2}K_4{}^{PhS} = 40.2 \pm 5$ dm^3 mol^{-1} and we know from the studies in the presence of $[pyrH]^+$ that ${}^{Fe2}K_4{}^{PhS}({}^{Fe2}k_5{}^{PhS})$

Table 1. Summary of the Rate Constants for the Proton-Transfer Reactions of Synthetic Fe−S-Based Clusters with $[pyrH]^+$

		transfer of nucleophile		transfer of proton	
		binding	dissociation		
cluster	pK_a	$^{M}k_4^{PhS}$/dm^3 mol^{-1} s^{-1}	$^{M}k_{-4}^{PhS}$/s^{-1}	$^{M}k_5^{PhS}$/dm^3 mol^{-1} s^{-1}	$^{M}k_1$/dm^3 mol^{-1} s^{-1}
		cuboidal			
$[Fe_4S_4Cl_4]^{2-}$ [5a]	18.8	1.4×10^5	2.2×10^5	1.8×10^6	2.4×10^4
$[\{MoFe_3S_4Cl_3\}_2(\mu\text{-SEt})_3]^{3-}$ [5b]	18.6	3.3×10^5	1.3×10^5	6.0×10^6	2.5×10^2
$[\{MoFe_3S_4Cl_3\}_2(\mu\text{-SPh})_3]^{3-}$ [5b]		3.8×10^5	1.3×10^5	1.6×10^6	5.0×10^2
		binuclear			
$[Fe_2S_2Cl_4]^{2-}$	18.1	a		$(2.5 \pm 0.3) \times 10^3$	$(1.8 \pm 0.2) \times 10^3$
$[S_2MoS_2FeCl_2]^{2-}$	17.9	2.0×10^5 [11]		$(1.0 \pm 0.2) \times 10^5$	$(3.4 \pm 0.6) \times 10^3$
$[S_2WS_2FeCl_2]^{2-}$	18.1			$(2.2 \pm 0.2) \times 10^5$	$(4.0 \pm 0.5) \times 10^3$

[a] Value of $^{Fe2}K_4^{PhS} = {}^{Fe2}k_4^{PhS}/{}^{Fe2}k_{-4}^{PhS} = 40.2$ dm^3 mol^{-1}.

$= (1.0 \pm 0.3) \times 10^5$ dm^6 mol^{-2} s^{-1}, we can calculate that $(^{Fe2}k_5^{PhS})/(^{Fe2}k_1) = 1.4$, indicating that addition of thiolate to the cluster has only a small effect on the rate of proton transfer. That binding thiolate to the cluster facilitates the rate of proton transfer is consistent with analogous studies on $[Fe_4S_4Cl_4]^{2-}$ and $[\{MoFe_3S_4Cl_3\}_2(\mu\text{-SEt})_3]^{3-}$. However, the effect observed with $[Fe_2S_2Cl_4]^{2-}$ is much smaller than that with the cuboidal clusters (see Table 1).

Rates of Proton Transfer to $[S_2MS_2FeCl_2]^{2-}$ (M = Mo or W). The kinetics of substitution of the first chloro group of $[S_2MS_2FeCl_2]^{2-}$ (M = Mo or W) with $[pyrH]^+$ in the presence of Br^- are simple and show the same behavior as the analogous reaction with $[Fe_2S_2Cl_4]^{2-}$. Thus, the rates of the reactions exhibit a first-order dependence on the concentrations of both cluster and $[pyrH]^+$ but are independent of the concentration of Br^-, as shown in Figure 8, for M = Mo.

The reactions of $[S_2MS_2FeCl_2]^{2-}$ with $[pyrH]^+$ in the presence of Br^- are associated with the rate law shown in eq 7 with $^{Mo}k_1 = (3.4 \pm 0.6) \times 10^3$ dm^3 mol^{-1} s^{-1} and $^{W}k_1 = (4.0 \pm 0.5) \times 10^3$ dm^3 mol^{-1} s^{-1}. Equation 7 is directly analogous to eqs 1 and 3 for the reactions of $[Fe_2S_2Cl_4]^{2-}$.

$$\frac{-\mathrm{d}[S_2MS_2FeCl_2^{2-}]}{\mathrm{d}t} = {}^{M}k_1[pyrH^+][S_2MS_2FeCl_2^{2-}] \quad (7)$$

On the other hand, the kinetics of the reactions of $[S_2MS_2FeCl_2]^{2-}$ with $[pyrH]^+$ in the presence of PhS^- are different than those observed in the analogous reactions of $[Fe_2S_2Cl_4]^{2-}$ described above. The rates of the reactions exhibit a first-order dependence on the concentration of cluster and a nonlinear dependence on the concentration of $[pyrH]^+$ but are independent of the concentration of PhS^-. As an illustration, the data for the reaction of $[S_2MoS_2FeCl_2]^{2-}$ with PhS^- in the presence of $[pyrH]^+$ are presented in Figure 9. Comparison of the data in Figures 8 and 9 shows that over the same concentration range of $[pyrH^+]$, the rates of the reactions in the presence of PhS^- are appreciably faster than those in the presence of Br^-.

Although the kinetics of the reactions of $[Fe_2S_2Cl_4]^{2-}$ and $[S_2MS_2FeCl_2]^{2-}$ with $[pyrH]^+$ in the presence of PhS^- are different, we propose that the mechanisms of the reactions are similar. Earlier studies[11] on the substitution reaction of $[S_2MoS_2FeCl_2]^{2-}$ with PhS^- showed that thiolate binds rapidly ($^{MoFe}k_4^{PhS} = 2.0 \times 10^5$ dm^3 mol^{-1} s^{-1}) to the cluster and, probably, to the Mo site. Consequently, in the reaction between $[S_2MS_2FeCl_2]^{2-}$ and $[pyrH]^+$ in the presence of PhS^-, the thiolate has bound to the cluster within the dead time of the stopped-flow apparatus (ca. 2 ms). Previously, it has been shown that in the reaction of PhS^- with $[S_2MoS_2FeCl_2]^{2-}$, in the absence of acid, binding of PhS^- to $[S_2MoS_2FeCl_2]^{2-}$ is associated with a small absorbance decrease.[11] In the absorbance−time curves associated with the reaction of $[S_2MoS_2FeCl_2]^{2-}$ with PhS^- in the presence of $[pyrH]^+$ the initial absorbance was not reproducibly significantly different than that of the parent cluster. We suggest that, in the presence of $[pyrH]^+$, the small initial absorbance decrease is not so evident as it is in the absence of acid because the reaction of $[pyrH]^+$ with $[(PhS)S_2MoS_2FeCl_2]^{3-}$ ($^{MoFe}k_5 = 1.0 \times 10^5$ dm^3 mol^{-1} s^{-1}) is appreciably faster than the reaction of PhS^- with $[(PhS)S_2MoS_2FeCl_2]^{3-}$ ($k = 6.4 \times 10^2$ dm^3 mol^{-1} s^{-1}).[11] Thus, the kinetics shown in Figure 9 correspond to those of the cluster with the thiolate already bound (i.e., $[(PhS)S_2MoS_2FeCl_2]^{3-}$). The mechanism of the reaction of $[S_2MS_2FeCl_2]^{2-}$ with PhS^- in the presence of $[pyrH]^+$ is shown in Figure 10. The binding of PhS^- is rapid, and consequently, at low concentrations of $[pyrH]^+$, protonation of $[(PhS)S_2MoS_2FeCl_2]^{3-}$ is rate limiting, and the initial linear slope of the curve shown in Figure 9 gives the rate constant for proton transfer ($^{MoFe}k_5^{PhS}$) presented in Table 1. We propose that the nonlinear dependence on the concentration of $[pyrH]^+$ shown in Figure 9 is attributable to a change in the rate-limiting step. Thus, at high concentrations of $[pyrH]^+$ the rate of proton transfer ($^{MoFe}k_5^{PhS}[pyrH^+]$) exceeds the rate of dissociation of the Fe−Cl bond ($^{MoFe}k_7^{PhS}$), and so the unimolecular step becomes rate limiting ($^{MoFe}k_7^{PhS} = 110 \pm 10$ s^{-1}; $^{WFe}k_7^{PhS} = 147 \pm 12$ s^{-1}). An analogous behavior involving change in the rate-limiting step has been observed previously[5] in the reaction of $[Fe_4S_4Cl_4]^{2-}$ with $[pyrH]^+$ in the presence of Br^-.

Kinetic Characteristics of Proton-Transfer Reactions to Synthetic Clusters. The studies measuring the rates of proton transfer to synthetic Fe−S-based clusters that have been performed to date[5] with $[pyrH]^+$ (including those described herein) show that the rates of the thermodynamically unfavorable reactions are characterized by the following features. (i) The rates are affected by the metal composition of the cluster. Earlier studies with Mo-containing cuboidal

(11) Gronberg, K. L. C.; Henderson, R. A.; Oglieve, K. E. *J. Chem. Soc., Dalton Trans.* **1997**, 1507.

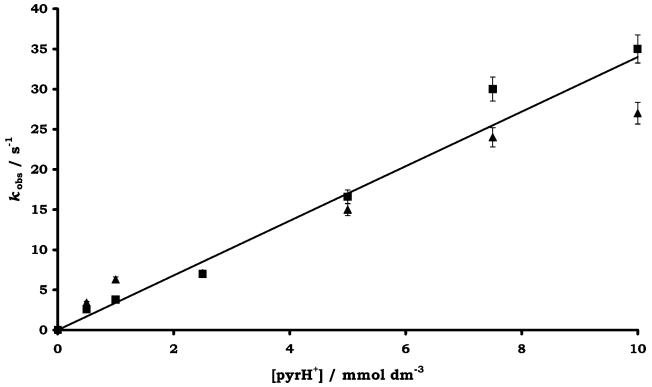

Figure 8. Kinetics of the reaction between $[S_2MoS_2FeCl_2]^{2-}$ (0.1 mmol dm^{-3}) and Br^- in the presence of $[pyrH]^+$ in MeCN at 25.0 °C. Data show the dependence of k_{obs} on the concentration of $[pyrH]^+$. The data points correspond to $[Br^-] = 5$ (▲) and 10 mmol dm^{-3} (■). Error bars indicate ±5% reproducibility. Line drawn is that defined by eq 7 and the rate constant presented in the text.

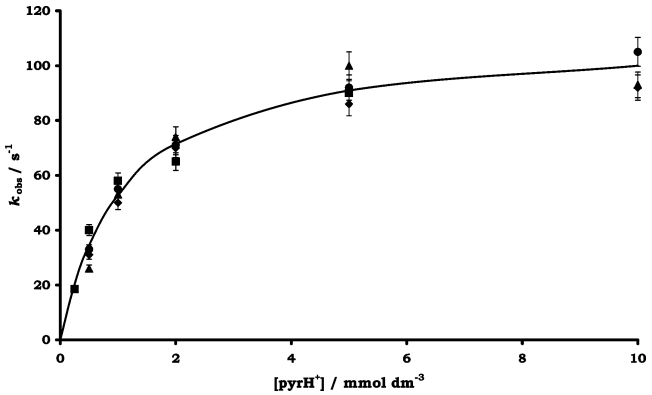

Figure 9. Kinetics of the reaction between $[S_2MoS_2FeCl_2]^{2-}$ (0.1 mmol dm^{-3}) and PhS^- in the presence of $[pyrH]^+$ in MeCN at 25.0 °C. Data show the dependence of k_{obs} on the concentration of $[pyrH]^+$. The data points correspond to $[PhS^-] = 2$ (◆), 5 (■), 10 (▲), and 20 mmol dm^{-3} (●). Error bars indicate ±5% reproducibility.

clusters indicated that these clusters protonate 50−100 times slower than Fe-only cuboidal cluster. However, the studies presented herein on binuclear systems show that this behavior is not general. Thus, while there is a 100-fold difference[5b] in the rates of proton transfer to $[Fe_4S_4Cl_4]^{2-}$ and $[\{MoFe_3S_4Cl_3\}_2(\mu\text{-}SR)_3]^{3-}$, the rates of proton transfer to $[Fe_2S_2Cl_4]^{2-}$ and $[S_2MoS_2FeCl_2]^{2-}$ differ only by a factor of 1.9. (ii) The rate of proton transfer is sensitive to the nature of the terminal ligands, and in systems where we have been able to measure the effect, binding of a nucleophile (PhS^-) to the cluster prior to proton-transfer results in an increased rate of proton transfer to the cluster. However, we wish to point out that recent studies indicate that this reactivity pattern may not be entirely general, and in some cases binding of a nucleophile can lead to a decrease in the rate of proton transfer to the cluster.[12] (iii) Although the kinetics are unambiguously those associated with proton transfer from $[pyrH]^+$ to the cluster, no measurable kinetic isotope effect has been observed[5] in the reactions with $[pyrD]^+$. It has been proposed that the absence of a significant primary isotope effect is a consequence of bond length reorganization within the entire cluster being a significant contributor to the activation process for proton transfer to Fe−S-based clusters. This proposal is consistent with the observation that electron-withdrawing 4-R-substituents on the coordinated thiolate in $[Fe_4S_4Cl_4(SC_6H_4R\text{-}4)]^{3-}$ leads to an increased rate of proton transfer to this intermediate.[13] On the basis of purely electronic effects it might be expected that electron-withdrawing 4-R-substituents would decrease the rate of proton transfer to the cluster by making the site less basic.

Parenthetically, it is worth noting that it would be anticipated for thermodynamically unfavorable proton-transfer reactions that the rates would be affected by the pK_a of the cluster.[14] However, because the rate of proton transfer to Fe−S-based clusters is sensitive to the nuclearity, terminal ligands, and metal composition we have not been able to establish this feature yet.

To further characterize the proton-transfer reactions of synthetic Fe−S-based clusters, the effect that temperature has on the rates of proton transfer has been investigated. The values of $\Delta H^{\ddagger}$ and $\Delta S^{\ddagger}$ determined with a range of Fe−S-based clusters are summarized in Table 2, and the correlation between $\Delta H^{\ddagger}$ and $\Delta S^{\ddagger}$ is shown in Figure 11. We are conscious that the apparent correlation shown in Figure 11 may not be real. As has been pointed out,[15] such "isokinetic plots" may only represent the errors in estimating $\Delta H^{\ddagger}$ and $\Delta S^{\ddagger}$ from a series of experiments over a relatively narrow temperature range. We believe that the apparent correlation in Figure 11 is not real for the reasons outlined below.

The data in Figure 11 shows that the proton-transfer reactions from $[pyrH]^+$ to cluster are all associated with a

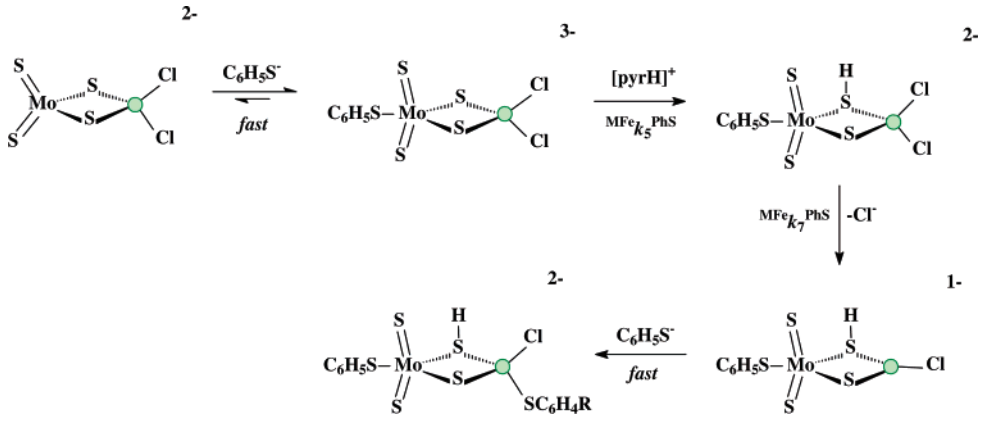

Figure 10. Mechanism of the reaction between $[S_2MoS_2FeCl_2]^{2-}$ and PhS^- in the presence of $[pyrH]^+$.

Table 2. Summary of the Activation Parameters for Proton Transfer

	pK_a	$\Delta H^{\ddagger}$/kcal mol^{-1}	$\Delta S^{\ddagger}$/cal deg^{-1} mol^{-1}
	cuboidal		
$[Fe_4S_4Cl_4]^{2-}$ [5b]	18.8	0.45 ± 0.2	−47 ± 5
$[Fe_4Se_4Cl_4]^{2-}$	19.3	4.25 ± 0.5	−26 ± 5
$[\{MoFe_3S_4Cl_3\}_2(\mu\text{-SEt})_3]^{3-}$ [5b]	18.6	0.0 ± 0.2	−65 ± 27
	binuclear		
$[Fe_2S_2Cl_4]^{2-}$	18.1	3.8 ± 0.5	−39 ± 5
$[S_2MoS_2FeCl_2]^{2-}$	17.9	4.8 ± 0.5	−27 ± 5
$[S_2WS_2FeCl_2]^{2-}$	18.1	5.3 ± 0.5	−24 ± 5

relatively small $\Delta H^{\ddagger}$ (0 to 5.3 kcal mol^{-1}) and a significantly negative $\Delta S^{\ddagger}$ (−24 to −65 cal deg^{-1} mol^{-1}). Furthermore, those reactions associated with a low $\Delta H^{\ddagger}$ have a correspondingly more negative $\Delta S^{\ddagger}$. This feature would be consistent with a description of the transition state between the $[pyrH]^+$ and cluster where the acid and cluster are close together and the transfer of the proton from the acid to the sulfur on the cluster is associated with a low barrier ($\Delta H^{\ddagger}$) with a correspondingly very negative $\Delta S^{\ddagger}$ (i.e., the transition state is product-like with the equilibrium position of the proton biased toward the sulfur). Similarly, those reactions with a larger barrier ($\Delta H^{\ddagger}$) are associated with a correspondingly less negative $\Delta S^{\ddagger}$ indicating a transition state which is reactant-like with the proton still principally associated with the $[pyrH]^+$. A similar description has been presented for the transition state associated with intramolecular proton transfer in the reactions of nickel−thiolate complexes hydrogen bonded to acids.[16] However, if the activation parameters shown in Figure 11 did indicate such a spectrum of transition state types for the proton-transfer reactions, it might be anticipated that there was a correlation of $\Delta H^{\ddagger}$ and $\Delta S^{\ddagger}$ with the pK_a's of the clusters since the pK_a is a measure of the affinity of the cluster for the proton. There is no such correlation of rates of proton transfer with the pK_as of the clusters. It is worth noting in Table 2 that proton transfer to clusters with essentially the same pK_a has very different activation parameters. For example, $[S_2WFeS_2Cl_2]^{2-}$ and $[Fe_2S_2Cl_4]^{2-}$ both have pK_a = 18.1 but quite different values of $\Delta H^{\ddagger}$ and $\Delta S^{\ddagger}$. Furthermore, proton transfer to $[Fe_4Se_4Cl_4]^{2-}$ (pK_a = 19.3) and $[S_2MoS_2FeCl_2]^{2-}$ (pK_a = 17.9), which have very different pK_as, has essentially the same values of $\Delta H^{\ddagger}$ and $\Delta S^{\ddagger}$.

We conclude that the plot shown in Figure 11 only indicates that the activation parameters derived from measuring the effect of temperature on the rates of proton transfer are essentially all the same with $\Delta H^{\ddagger} = 3.0 \pm 3.0$ kcal mol^{-1} and $\Delta S^{\ddagger} = -44 \pm 21$ cal deg^{-1} mol^{-1}. The small value of $\Delta H^{\ddagger}$ is consistent with earlier proposals that the transition state for proton transfer is associated with low activation

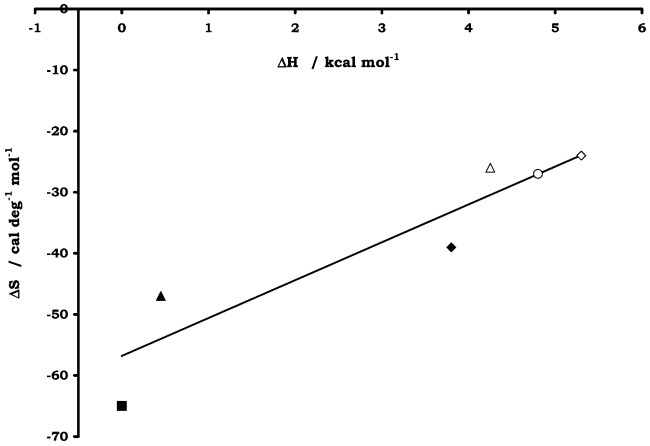

Figure 11. Apparent isokinetic plot for the activation parameters for the proton-transfer reactions of synthetic Fe-S-based clusters. Data points correspond to $[Fe_4S_4Cl_4]^{2-}$ (▲)[5b], $[\{MoFe_3S_4Cl_3\}_2(\mu\text{-SEt})_3]^{3-}$ (■)[5b], $[Fe_4Se_4Cl_4]^{2-}$ (△), $[Fe_2S_2Cl_4]^{2-}$ (◆), $[S_2MoS_2FeCl_2]^{2-}$ (○), and $[S_2WS_2FeCl_2]^{2-}$ (◇). The line drawn is that defined by the relationship $\Delta S^{\ddagger} = 6.2(\Delta H^{\ddagger}) - 56.8$.

enthalpy. The negative $\Delta S^{\ddagger}$ is consistent with a transition state with increased order where the cluster and $[pyrH]^+$ form an adduct prior to intramolecular transfer of the proton within the adduct.[17]

Rates of Proton Transfer in Synthetic Clusters: Some General Considerations. All of the reactions of synthetic Fe−S-based clusters with $[pyrH]^+$, in the presence of the nucleophiles PhS^- or Br^-, presented in this paper occur by the pathways shown in Figure 4, and analogous pathways have previously been shown to operate for cuboidal Fe−S-based clusters.[5b] The two pathways shown in Figure 4 differ only in the relative order that the nucleophile (Nu^-) and proton bind to the cluster. Irrespective of the cluster, two factors control which pathway operates for any cluster: (i) the relative rates of proton transfer and binding of Nu^- to the parent cluster and (ii) the affinity of Nu^- for the cluster.

The studies on proton-transfer rates to synthetic Fe−S-based clusters reported to date[4b,5] (summarized in Table 1) indicate that the rates of thermodynamically unfavorable proton transfer show a marked dependence on the composition of the cluster. We can also calculate[18] the rate constant for the thermodynamically favorable proton transfer from the protonated cluster to [pyr] using $^{M}K_1$ (calculated using the pK_a of the cluster and $[pyrH]^+$) and the measured value of $^{M}k_1$. For $[Fe_2S_2Cl_4]^{2-}$ and $[S_2MS_2FeCl_2]^{2-}$ (M = Mo or W), $^{M}k_{-1} = (0.7 \pm 0.3) \times 10^7$ dm^3 mol^{-1} s^{-1}. This value is consistent with earlier estimates of the maximum rates of proton transfer involving synthetic Fe−S-based clusters;[5a] for example, for $[Fe_4S_4Cl_4]^{2-}$ $\{^{Fe4}k_{-1} = 1.2 \times 10^7$ dm^3 mol^{-1} s$^{-1}\}$. It appears that the fastest rate at which a synthetic Fe−S-based cluster can be protonated in MeCN is ca. 1×10^7 dm^3 mol^{-1} s^{-1}.

(12) Bates, K.; Henderson, R. A. Unpublished work.
(13) Henderson, R. A.; Dunford, A. J. *Chem. Commun*. **2002**, 360.
(14) (a) Eigen, M. *Angew. Chem., Int. Ed*. **1964**, *3*, 1 and references therein. (b) Kramarz, K. W.; Norton, J. R. *Prog. Inorg. Chem*. **1994**, *42*, 1 and references therein. (c) Henderson, R. A. *Angew. Chem., Int. Ed*. **1996**, *35*, 946 and references therein.
(15) Cornish-Bowden, A. J. *J. Biosci*. **2002**, *27*, 121.
(16) Autissier, V.; Zarza, P. M.; Petrou, A.; Henderson, R. A.; Harrington, R. W.; Clegg, W. *Inorg. Chem*. **2004**, *43*, 3106.
(17) (a) Albery, W. J. *Annu. Rev. Phys. Chem*. **1980**, *31*, 227. (b) Albery, W. J. *Faraday Discuss. Chem. Soc*. **1982**, *74*, 245 and references therein.
(18) Bell, R. P. *The Proton in Chemistry*, 2nd ed.; Chapman & Hall: London, 1973; p 195.

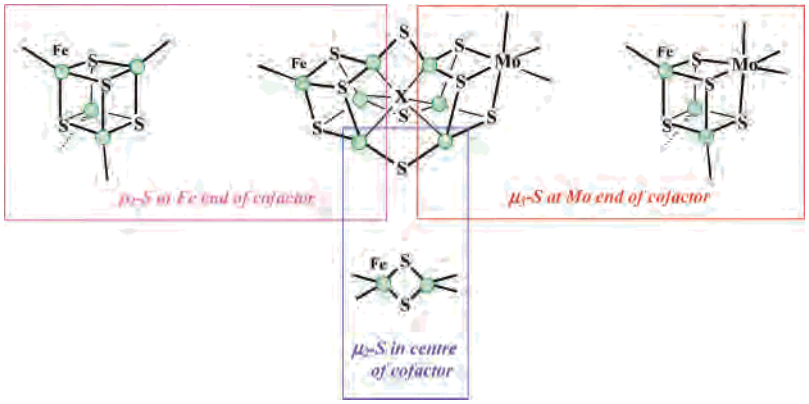

Figure 12. Representation of the FeMo-cofactor of the Mo-based nitrogenase and the synthetic Fe-S-based clusters whose structure mimics portions of the cofactor structure X = C, N, or O.

It is worth considering further the rate of proton transfer from $[pyrH]^+$ to $[Fe_2S_2Cl_4]^{2-}$. Inspection of Table 1 indicates that proton transfer from $[pyrH]^+$ to $[Fe_2S_2Cl_4]^{2-}$ (containing only μ_2-S) is apparently *slower* than proton transfer to $[Fe_4S_4Cl_4]^{2-}$ (containing only μ_3-S), $^{Fe4}k_1 = 13(^{Fe2}k_1)$. However, in interpreting this difference it is important to appreciate that there is a difference in basicities of the two clusters, $^{Fe4}K_a = 5.0(^{Fe2}K_a)$. If we correct for the different thermodynamic driving forces for the proton transfer from $[pyrH]^+$ to $[Fe_2S_2Cl_4]^{2-}$ and $[Fe_4S_4Cl_4]^{2-}$, the difference in rates of proton transfer to the two clusters is small $[^{Fe4}k_1 = 2.6(^{Fe2}k_1)]$. Furthermore, the ligation of the cluster is also an important feature in controlling the rates of proton transfer to synthetic Fe−S-based clusters (vide infra). Thus, at least part of the difference in the rates of proton transfer to these two clusters may be attributable to the μ_2-S being bound to two $FeCl_2$ residues while the μ_3-S is bound to three FeCl residues.

The data presented in Table 1 allows us to compare the rate of proton transfer to the parent cluster ($^{M}k_1$) with the rate of proton transfer to the cluster with PhS^- bound ($^{M}k_5^{PhS}$). It is evident from the studies performed to date that prior binding of PhS^- to the cluster facilitates proton transfer. However, the effect that binding PhS^- has on the rates of proton transfer to the cluster is markedly dependent on the composition and nuclearity of the cluster: $[Fe_4S_4Cl_4]^{2-}$ $\{(^{Fe4}k_5^{PhS})/(^{Fe4}k_1) = 75\}$; $[\{MoFe_3S_4Cl_3\}_2(\mu\text{-SEt})_3]^{3-}$ $\{(^{MoFe3}k_5^{PhS})/(^{MoFe3}k_1) = 25000\}$; $[\{MoFe_3S_4Cl_3\}_2(\mu\text{-SPh})_3]^{3-}$ $\{(^{MoFe3}k_5^{PhS})/(^{MoFe3}k_1) = 3200\}$; $[Fe_2S_2Cl_4]^{2-}$ $\{(^{Fe2}k_5^{PhS})/(^{Fe2}k_1) = 1.4\}$; $[S_2MoS_2FeCl_2]^{2-}$ $\{(^{MoFe}k_5^{PhS})/(^{MoFe}k_1) = 29.4\}$; $[S_2WS_2FeCl_2]^{2-}$ $\{(^{WFe}k_5^{PhS})/(^{WFe}k_1) = 55\}$. It has also been observed[5c] that the binding of Bu^tNC to $[Fe_4S_4Cl_4]^{2-}$ increases the rate of protonation by $[pyrH]^+$, but in this case, the increase in rate cannot be quantified.

Rates of Proton Transfer in Natural Fe−S-Based Clusters. The work presented in this paper (on synthetic Fe−S-based clusters) allows us, for the first time, to discuss likely protonation sites for the natural clusters based on kinetic and thermodynamic measurements on the protonation of synthetic Fe−S-based clusters. In particular our studies indicate that there may be little difference in both the basicities and the rates of proton transfer to μ_2-S and μ_3-S.

Fe−S-based clusters comprise at least part of the active site in a wide range of proteins. In most the natural cluster contains either μ_3-S or μ_2-S. However, the FeMo-cofactor of nitrogenase[19] and the $\{Fe_3S_4\}$ cluster of Ferredoxin I from *Azotobacter vinelandii*[20] contain both μ_3-S and μ_2-S, and it is the protonation sites of these clusters which we will consider further.

A number of papers have explored possible mechanisms for the conversion of dinitrogen into ammonia at FeMo-cofactor using DFT calculations.[3,21] Since the mid-1990s to the present day a variety of such DFT-based mechanisms have proposed that protonation of the central μ_2-S sites is a prequel to production of dihydrogen or binding of dinitrogen. In some of the DFT studies the calculations indicated that hydrogen atoms bind more strongly to μ_2-S than μ_3-S, but in other studies protonation of the μ_2-S is just considered "most likely".

The structural characteristics of synthetic Fe−S-based clusters make them adequate (but incomplete) models for portions of the FeMo-cofactor, as indicated in Figure 12. At an admittedly somewhat crude level, the μ_2-S in binuclear clusters and μ_3-S in cuboidal clusters are models for the corresponding sites in FeMo-cofactor. The work described in this paper together with that reported earlier for the cuboidal $\{Fe_4S_4\}$ and $\{MoFe_3S_4\}$ clusters indicate that on both thermodynamic (basicity) and kinetic considerations (rates of proton transfer) there is no significant distinction in the quantitative protonation chemistry of the μ_2-S and μ_3-S sites. In particular, our studies on the protonation of the synthetic clusters indicate that (i) the rates of protonation of all sulfurs in cofactor would be slower than the diffusion-controlled limit, (ii) the rates of protonation of the μ_2-S and μ_3-S sites in FeMo-cofactor could also be very similar, differing by less than a factor of 10, and (iii) there may be little difference in the basicities of μ_2-S and μ_3-S sulfur sites.

The $\{Fe_3S_4\}$ voided cuboidal cluster of Ferredoxin I from *Azotobacter vinelandii* has an unusually low, pH-dependent,

(19) Einsle, O.; Teczan, F. A.; Anstrade, S.; Schmid, B.; Yoshida, M.; Howard, J. B.; Rees, D. C. *Science* **2002**, *297*, 1696 and references therein.
(20) (a) Stout, C. D. *J. Biol. Chem.* **1988**, *263*, 9256. (b) Stout, C. D. *J. Mol. Chem.* **1989**, *205*, 545.
(21) Rodd, T. H.; Nørskov, J. K. *J. Am. Chem. Soc.* **2000**, *122*, 12751.

reduction potential.[22] The protein transfers two electrons, and it was concluded that after transfer of one electron protonation occurs directly at the cluster before the second electron transfer can occur. It was proposed that one of the μ_2-S atoms in $\{Fe_3S_4\}$ is the most likely site of protonation.[22] Clearly, in order that addition of the second electron is not impeded, the rate of the protonation step must be fast. The work presented in this paper indicates, contrary to what might be intuitive, that the μ_2-S atoms and the unique μ_3-S might have similar proton affinties and be protonated at similar rates.

Experimental Section

All manipulations were routinely performed under an atmosphere of dinitrogen using standard Schlenk or syringe techniques as appropriate. All solvents were dried and distilled under dinitrogen immediately prior to use. Acetonitrile was distilled from calcium hydride and methanol from $Mg(OMe)_2$. Tetrahydrofuran and diethyl ether were dried in a two-stage process; the bulk of water was removed by adding sodium to the solvent as supplied, and then the predried solvents were distilled over sodium/benzophenone or sodium, respectively. Ethanol was used as received.

NMR spectra were recorded on a 300 MHz Bruker NMR spectrometer fitted with a wide bore cavity to hold larger NMR tubes operating at 121.5 MHz.

The following chemicals were purchased from Aldrich and used as received: $FeCl_2$, $FeCl_3$, NEt_3, pyr (pyr = pyrrolidine), C_6H_5SH, $Na[BPh_4]$, $[NH_4]_2MoS_4$, $[NH_4]_2WS_4$, $[NBu^n_4]Br$, $(Me_3Si)_2S$, Na, S_8, Me_3SiCl, and PhCOCl.

$[NEt_4]Cl{\cdot}H_2O$ and $[NEt_4]Br$ were purchased from Aldrich and dried prior to use by heating and stirring at 80 °C in vacuo for 5 h.

The following clusters were prepared by the methods described in the literature and characterized by elemental analysis and comparison of the UV−vis spectrum with that in the literature. $[NEt_4]_2[Fe_2S_2Cl_4]$[23] (λ_{max} = 357 nm, ϵ_{max} = 3880 dm^3 mol^{-1} cm^{-1}; λ_{max} = 455 nm, ϵ_{max} = 3000 dm^3 mol^{-1} cm^{-1}; λ_{max} = 571 nm, ϵ_{max} = 1720 dm^3 mol^{-1} cm^{-1})[24] $[PPh_4]_2[S_2MoS_2FeCl_2]$[25] ($\lambda_{max}$ = 432 nm, ϵ_{max} = 4800 dm^3 mol^{-1} cm^{-1}; λ_{max} = 469 nm, ϵ_{max} = 6400 dm^3 mol^{-1} cm^{-1}),[26] $[PPh_4]_2[S_2W_2S_2FeCl_2]$[27] ($\lambda_{max}$ = 380 nm, ϵ_{max} = 5000 dm^3 mol^{-1} cm^{-1}; λ_{max} = 420 nm, ϵ_{max} = 4500 dm^3 mol^{-1} cm^{-1}; λ_{max} = 520 nm, ϵ_{max} = 1200 dm^3 mol^{-1} cm^{-1}).[28]

The acids and $[NEt_4]SPh$ were prepared by the literature methods and characterized by elemental analysis (calculated values in parentheses) and ^{1}H NMR spectroscopy. $[NHEt_3]BPh_4$: C, 85.6 (85.5); H, 8.70 (8.61); N, 3.28 (3.32); NMR δ 1.2 (t, CH_3), 3.03 (q, CH_2), 6.3 (br, NH), 6.9−7.3 (m, Ph).[29] $[pyrH]BPh_4$: C, 86.0 (85.9); H, 7.6 (7.7); N, 3.6 (3.6); NMR δ 1.9 (m, CH_2CH$_2$N), 3.20 (t, CH$_2$CH_2N, J_{HH} = 7.5 Hz), 6.6 (br, NH_2), 6.8−7.3 (m, Ph).[5b] $[NEt_4]SPh$: C, 71.0 (70.3); H, 10.5 (10.5); N, 5.7 (5.9); NMR δ 1.2 (t, CH_3), 3.1 (q, CH_2), 6.6−7.2 (m, Ph)}.[30]

The products of the reaction between $[Fe_2S_2Cl_4]^{2-}$ and PhS^- have previously been shown to be $[Fe_2S_2(SPh)_4]^{2-}$ by both ourselves[31] and other workers.[24] $[Fe_2S_2(SPh)_4]^{2-}$ was not isolated from the reaction, but the visible absorption spectrum of the final reaction solution was identical to that of $[Fe_2S_2(SPh)_4]^{2-}$ reported in the literature[32] (λ_{max} = 335 nm (shoulder), ϵ_{max} = 2.0 × 10^4 dm^3 mol^{-1} cm^{-1}; λ_{max} = 495 nm, ϵ_{max} = 1.1 × 10^4 dm^3 mol^{-1} cm^{-1}).

The visible spectrum of the final reaction mixture of the reaction between $[Fe_2S_2Cl_4]^{2-}$ and Br^- is consistent with the product being $[Fe_2S_2Br_4]^{2-}$ (λ_{max} = 370 nm, ϵ_{max} = 8.5 × 10^3 dm^3 mol^{-1} cm^{-1}; λ_{max} = 420 nm (shoulder), ϵ_{max} = 2.9 × 10^3 dm^3 mol^{-1} cm^{-1}; λ_{max} = 480 nm (shoulder), ϵ_{max} = 4.6 × 10^3 dm^3 mol^{-1} cm^{-1}; λ_{max} = 600 nm, ϵ_{max} = 2.5 × 10^3 dm^3 mol^{-1} cm^{-1}) and is essentially the same as that reported in the literature.[24] The reaction between $[Fe_2S_2Cl_4]^{2-}$ and Br^- in the presence of $[pyrH]^+$ needs to be studied at low wavelengths (λ = 400 nm) since at higher wavelengths the difference in absorbance between $[Fe_2S_2Cl_4]^{2-}$ and $[Fe_2S_2Br_4]^{2-}$ is too small to measure at low concentrations of cluster.

The products of the reactions between $[S_2MS_2FeCl_2]^{2-}$ (M = Mo or W) and PhS^- have previously been shown by ourselves[11] and others[26] to be $[S_2MS_2Fe(SPh)_2]^{2-}$. The visible spectrum of the products were in good agreement with those reported in the literature[33] (for M = Mo: λ_{max} = 550 nm (shoulder), $\epsilon_{max} \approx$ 4 × 10^3 dm^3 mol^{-1} cm^{-1}; λ_{max} = 485 nm, ϵ_{max} = 9.0 × 10^3 dm^3 mol^{-1} cm^{-1}; λ_{max} = 430 nm, ϵ_{max} = 8.1 × 10^3 dm^3 mol^{-1} cm^{-1}; for M = W: λ_{max} = 550 nm (shoulder), $\epsilon_{max} \approx$ 1.6 × 10^3 dm^3 mol^{-1} cm^{-1}; λ_{max} = 430 nm, ϵ_{max} = 4.6 × 10^3 dm^3 mol^{-1} cm^{-1}; λ_{max} = 350 nm, ϵ_{max} = 5.8 × 10^3 dm^3 mol^{-1} cm^{-1}).

The products of the reactions between $[S_2MS_2FeCl_2]^{2-}$ and Br^- are (reasonably) assumed to be $[S_2MS_2FeBr_2]^{2-}$. Although we were unable to isolate the products, synthesis of $[S_2WS_2FeCl_2]^{2-}$ (but not $[S_2MoS_2FeCl_2]^{2-}$) has been reported.[34] The visible absorption spectrum of the products are very similar to those of $[S_2MS_2FeCl_2]^{2-}$ except in general they are more intensely absorbing. For $[S_2MoS_2FeCl_2]^{2-}$: λ_{max} = 440 nm (shoulder), ϵ_{max} = 5.2 × 10^3 dm^3 mol^{-1} cm^{-1}; λ_{max} = 469 nm, ϵ_{max} = 7.0 × 10^3 dm^3 mol^{-1} cm^{-1}. For $[S_2WS_2FeCl_2]^{2-}$: λ_{max} = 420 nm, ϵ_{max} = 5.2 × 10^3 dm^3 mol^{-1} cm^{-1}; λ_{max} = 540 nm, ϵ_{max} = 1.5 × 10^3 dm^3 mol^{-1} cm^{-1}.

Kinetic Studies. All kinetic studies were performed using an Applied Photophysics SX.18 MV stopped-flow spectrophotometer modified to handle air-sensitive solutions connected to a RISC pc. The temperature was maintained at 25.0 ± 0.1 °C using a Grant LTD 6G thermostat tank with combined recirculating pump. The solutions of cluster and reactants were prepared under an atmosphere of dinitrogen and transferred to the spectrophotometer via gastight, all-glass syringes. The solutions of all reagents were prepared by dilution from freshly made stock solutions in MeCN and used within 1 h.

The absorbance−time traces were fitted to exponential curves using the Applied Photophysics software. Typical stopped-flow absorbance−time traces together with curved fits are shown in Figure 2. The observed rate constants (k_{obs}) presented in the figures

(22) Hirst, J.; Duff, J. L. C.; Jameson, G. N. L.; Kemper, M. A.; Burgess, B. K.; Armstrong, F. A. *J. Am. Chem. Soc.* **1998**, *120*, 7085.
(23) Do, Y.; Simhon, E. D.; Holm, R. H. *Inorg. Chem.* **1983**, *22*, 3809.
(24) Wong, G. B.; Bobrik, M. A.; Holm, R. H. *Inorg. Chem.* **1978**, *17*, 578.
(25) Muller, A.; Tolle, H. G.; Bogge, H. *Z. Anorg. Allg. Chem.* **1980**, *471*, 115.
(26) Tiecklemann, R. H.; Silvis, H. C.; Kent, T. A.; Huynh, B. H.; Waszczak, J. V.; Teo, B. K.; Averill, B. A. *J. Am. Chem. Soc.* **1980**, *102*, 5550.
(27) Coucouvanis, D.; Simhon, E. D.; Stremple, P.; Ryan, M.; Swenson, D.; Baenziger, N. C.; Simopoulos, A.; Papaefthymiou, V.; Kostikas, A.; Petrouleas, V. *Inorg. Chem.* **1984**, *23*, 741.
(28) Muller, A.; Jostes, R.; Tölle, H. G.; Trautwein, A.; Bill, E. *Inorg. Chim. Acta* **1980**, *46*, L121.
(29) Dilworth, J. R.; Henderson, R. A.; Dahlstrom, P.; Nicholson, T.; Zubieta, J. A. *J. Chem. Soc., Dalton Trans.* **1987**, 529.
(30) Palermo, R. E.; Power, P. P.; Holm, R. H. *Inorg. Chem.* **1982**, *21*, 173.
(31) Garrett, B.; Henderson, R. A. *Dalton Trans.* **2007**, 3435.
(32) Mayerle, J. J.; Denmark, S. E.; DePamphilis, B. V.; Ibers, J. A.; Holm, R. H. *J. Am. Chem. Soc.* **1975**, *97*, 1032.
(33) Coucouvanis, D.; Stremple, P.; Simhon, E. D.; Swenson, D.; Baenziger, N. C.; Draganjac, M.; Chan, L. T.; Simopoulos, A.; Papaefthymiou, V.; Kostikas, A.; Petrouleas, V. *Inorg. Chem.* **1983**, *22*, 293.
(34) Fedin, V. P.; Sokolov, M. N.; Ikorskii, V. N.; Fedorov, V. E. *Zh. Neorg. Khim.* **1989**, *34*, 3210.

are the average of at least three experiments. The error bars presented in Figures 3 (insert), 8, and 9 show the 5% reproducibility of these data, whereas in Figures 3 (main), 5 (main and insert), and 6 the error bars correspond to 10%, reflecting the greater uncertainty in determining k_{obs} from biphasic traces. All experiments were performed under pseudo-first-order conditions with the concentration of all reagents in an excess over the concentration of cluster.

Measurement of $\Delta H^{\ddagger}$ and $\Delta S^{\ddagger}$. The activation parameters ($\Delta H^{\ddagger}$ and $\Delta S^{\ddagger}$) for $[Fe_4S_4Cl_4]^{2-}$ and $[\{MoFe_3S_4Cl_3\}_2(\mu\text{-}SEt)_3]^{3-}$ have been reported earlier.[5b] For $[Fe_2S_2Cl_4]^{2-}$, $[S_2MS_2FeCl_2]^{2-}$ (M = Mo or W) and $[Fe_4Se_4Cl_4]^{2-}$ the activation parameters are reported herein for the first time and were determined by measuring the effect that temperature has on the rate of the protonation reactions. In all studies the temperature was varied over at least 20 °C, controlled using the thermostat tank. Typically, at each temperature the concentrations of the cluster and Br^- were kept constant and the concentration of $[pyrH]^+$ varied to determine the second-order rate constant ($^{M}k_1$) at each temperature. For $[Fe_2S_2Cl_4]^{2-}$ and $[S_2MS_2FeCl_2]^{2-}$ (M = Mo or W): [cluster] = 0.05 mmol dm^{-3}; [Br^-] = 10 mmol dm^{-3} and [$pyrH^+$] = 1 − 10 mmol dm^{-3}. For $[Fe_4Se_4Cl_4]^{2-}$: [cluster] = 0.2 mmol dm^{-3}; [Br^-] = 2.5 mmol dm^{-3} and [$pyrH^+$] = 10 − 80 mmol dm^{-3}.

The values of $\Delta H^{\ddagger}$ and $\Delta S^{\ddagger}$ for protonation of each cluster were determined using the Eyring equation[35] shown in eq 8. Plots of $\log(^{M}k_1/T)$ versus $1/T$ were straight lines, and unweighted linear least-squares fits of the data gave the value of $\Delta H^{\ddagger}$ (in cals) from the slope and the value of $\Delta S^{\ddagger}$ (in cals) from the intercept.

$$\log_{10}\left(\frac{^{M}k_1}{T}\right) = 10.32 - \frac{\Delta H^{\ddagger}}{4.57 \times 10^{-3}(T)} + \frac{\Delta S^{\ddagger}}{4.57} \qquad (8)$$

In the studies on $[Fe_4Se_4Cl_4]^{2-}$ there is a nonlinear dependence on the concentration of $[pyrH^+]$ (as described earlier for $[Fe_4S_4Cl_4]^{2-}$).[5b] In this case, the activation parameters shown in Figure 11 and Table 2 correspond to the temperature dependence of the reaction at low concentrations of $[pyrH]^+$, where there is a linear dependence on the concentration of $[pyrH]^+$ and proton transfer is rate limiting.

Acknowledgment. We thank the EPSRC for studentships to K.B. and B.G.

Supporting Information Available: Tables containing the observed rate constants for all reactions of $[Fe_2S_2Cl_4]^{2-}$ and $[S_2MS_2FeCl_2]^{2-}$ (M = Mo or W) and the temperature dependence of $[Fe_4Se_4Cl_4]^{2-}$. This material is available free of charge via the Internet at http://pubs.acs.org.

IC7015484

(35) Hussain, W.; Leigh, G. J.; Mohd Ali, H.; Pickett, C. J.; Rankin, D. A. *J. Chem. Soc., Dalton Trans.* **1984**, 1703 and references therein.